Sensors and Materials, Vol. 35, No. 3 (2023) 1149–1160
MYU Tokyo

S & M 3236

Factors Affecting Efficiency of Thrombolysis Using Magnetically Controlled Fe_3O_4 Nanoparticles

Qian Li[1*] and Zhen Lu[2]

[1]School of Mechanical Engineering, University of Shanghai for Science and Technology, Jungong Road 516, Shanghai 200093, China,
[2]College of Computer Science and Technology, Shanghai University of Electric Power, Changyang Road 2588, Shanghai 200090, China

(Received November 28, 2022; accepted March 1, 2023)

Keywords: Fe_3O_4 nanoparticles, thrombolysis efficiency, microfluidic channel, magnetic field

We report on thrombolysis using urokinase (UK)-coated Fe_3O_4 magnetic nanoparticles (MNPs) under an oscillating magnetic field in microfluidic channels under different conditions. With the help of a theoretical model and the multiphysics simulation software COMSOL, we analyzed the magnetic force and motion of the MNP aggregation in the oscillating magnetic field induced by an energized coil. On the basis of the steady flow theory, we analyzed the factors affecting the thrombolysis efficiency, such as the bending angle, the diameter of the microfluidic channel, the mass fraction of MNPs, and the strength of the magnetic field. Thrombolysis efficiency is considered an important factor in stroke therapy clinics because of strict time restrictions. The medium in a microfluidic channel will cause a rapid velocity with functionalized nanoparticle (NP) movement and rotation under an alternating field. Thus, an increased flow pressure will act on the target and accelerate the release of the enzyme or drug attached to the NPs to dissolve the thrombus chemically. *In vitro* experiments revealed that increases in the bending angle and diameter of the microfluidic channel result in a decrease in the efficiency of thrombolysis using UK-coated MNPs. The increase in the mass fraction of UK-coated MNPs results in a faster increase in thrombolysis efficiency than that of pure UK. The increase in the peak amplification of the oscillating magnetic field also improves the thrombolysis efficiency. The analysis of these factors can help sense the thrombolysis efficiency and enable doctors to make the right choices in clinical treatment.

1. Introduction

Owing to their good biocompatibility and noninvasive manipulation characteristics, magnetic nanomaterials have attracted researchers' interests given their applications in human biomedical difficulties, such as the catabolism of tumors by hyperthermia, drug delivery for targeting diseased tissues, and gene delivery.[1–4] One of the serious life-threatening illnesses is thrombus occlusion, which prevents blood flow and results in acute stroke and myocardial infarction. A number of enzymes such as urokinase (UK) and streptokinase have been discovered and

*Corresponding author: e-mail: LQ9365@sina.com
https://doi.org/10.18494/SAM4259

ISSN 0914-4935

extracted for thrombus ablation.[5–9] However, the necessarily frequent drug injection with large doses, which allows more of the drug to reach the lesion site, also aggravates the risk of hemorrhaging and worsen the situation for patients. The combination of magnetic nanoparticles (MNPs) and thrombolytic drugs can accelerate thrombolysis under a static magnetic field and an acoustic field more so than injected drugs.[10] According to Chang *et al.*, control over the actions of MNPs and the combination of drugs with MNPs may reduce the time of thrombolysis.[11] However, even if a short time is significant for the best therapy, seeking new and highly efficient thrombolysis methods is meaningful with the precondition that factors affecting the process should be analyzed. This work is an analysis of the factors that affect the efficiency of thrombolysis using UK-coated MNPs controlled by an alternating magnetic field, including the bending angle, the diameter of the microfluidic channel, and the strength of the alternating magnetic field. The remote sensing of the thrombolysis efficiency will consider these factors, which will help researchers further improve the thrombolysis rate in the clinical setting.

2. Theory and Fundamental Principles

2.1 Movement and rotation of MNPs under a magnetic field

Super-paramagnetic MNP colloids will form ellipsoid-like aggregations through a particle–particle magnetic attraction force under magnetic fields.[5] The lengths of the aggregations vary with time as the colloids attempt to reach an equilibrium state.[12] The magnetic force can be derived by reading reviews for details.[13] By considering an NP as a point-like magnetic dipole $\boldsymbol{m}$, the magnetic force $\boldsymbol{F}_m$ in the magnetic field $\boldsymbol{B}$ is given as

$$\boldsymbol{F}_m = \left(\boldsymbol{m}\cdot\nabla\right)\boldsymbol{B}. \tag{1}$$

For the aggregation of NPs, the total moment on the particles can be written as $\boldsymbol{m} = V_m\boldsymbol{M}$, where V_m is the volume of the aggregation and $\boldsymbol{M}$ is the volumetric magnetization, which is given by $\boldsymbol{M} = \Delta\chi\boldsymbol{H}$ with $\Delta\chi = \chi_m - \chi_w$ being the effective susceptibility of the NPs in water. According to the following identity $\nabla\left(\boldsymbol{B}\cdot\boldsymbol{B}\right) = 2\left(\boldsymbol{B}\cdot\nabla\right)\boldsymbol{B}$, derived from the Maxwell equation $\nabla\times\boldsymbol{B} = 0$, the magnetic force of the aggregation can be shown as

$$\boldsymbol{F}_{magg} = \frac{B^2\Delta\chi V_m}{2\mu_0}\nabla. \tag{2}$$

The magnetic force will result in the movement of the aggregation. When the aggregation moves in water, it will experience fluidic resistance. According to Stoke's formula, such a force is proportional to the moving velocity, $\boldsymbol{F}_d = \gamma\boldsymbol{v}$. Provided that the aggregation is moving with a constant velocity, it can be evaluated as

$$\boldsymbol{v} = \frac{B^2 \Delta\chi V_m}{2\mu_0 \gamma} \nabla . \tag{3}$$

In the formula $\gamma = 6\pi\eta r$, r is the equivalent radius of the same volume and η is the viscosity of the medium.

The aggregation rotates around the easy magnetization axis of the NPs and is guided by the change in the direction of the magnetic field. In a medium with a low Reynolds number, the rotation speed can be obtained as[12]

$$\omega = \frac{3V_m \Delta\chi^2 H^2 \sin(2\theta)}{32(2+\Delta\chi)\pi\eta ab^2}, \tag{4}$$

where θ is the angle between the easy axis and the magnetic field. a and b are the lengths of the minor and major axes of the ellipsoid-like aggregation, respectively.

2.2 Steady laminar flow in a microfluidic channel with a bend

The medium in a microfluidic channel will apply pressure to the wall. When it flows across a bend, the pressure will suffer a sudden decrease.[14] The model of flow in a microfluidic channel with bending angle θ is described in Fig. 1. In the bend portion, the fluid near the axis of the duct having the highest velocity is subjected to a larger centrifugal force than the slower moving fluid in the neighborhood of the duct wall. The sudden change in velocity will induce a secondary flow perpendicular to the primary axial flow. As a result, the pressure in the piping system suffers a considerable decrease. The analysis of this situation is shown in Fig. 1. The pressure losses in the pipe change following the curve of *ABCD* without the bend *MN* and the curve of *ABEF* with the bend *MN*. Ward-Smith gave the coefficient K_b to describe the pressure loss. [15]

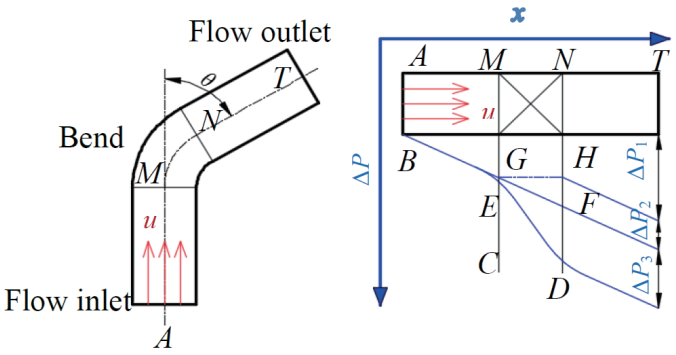

Fig. 1. (Color online) Schematic variation of centerline pressure with a bend.

$$K_b = \frac{\Delta P_2 + \Delta P_3}{\rho u^2 / 2} \tag{5}$$

$\Delta P_1$is the loss of pressure in a straight pipe. ΔP_2 is the pressure loss that is added owing to skin friction in the straightened length of the bend region. ΔP_3 is the pressure loss associated with wake friction due to the bend.

In the channel, thrombolysis will be carried out. The ellipsoid-like aggregations rotate in the oscillating magnetic field, which induces the flow of the blood to shock and damage the thrombus occlusion. At the same time, the UK coated on the MNPs will be released in the blood and pushed to come into contact with the thrombus. Thus, physical and chemical means are adopted simultaneously for thrombolysis.

3. Numerical Simulation

3.1 Magnetic force and motion of MNPs

We simulate the movement of the aggregation in oscillating fields for research using COMSOL5.0. The following equations were used to construct the model:

$$\frac{\partial \rho}{\partial t} + \nabla \cdot \left(\rho \boldsymbol{u} \right) = 0, \tag{6}$$

$$\rho \frac{\partial \boldsymbol{u}}{\partial t} + \rho \left(\boldsymbol{u} \cdot \nabla \right) \boldsymbol{u} = \nabla \cdot \left\{ -p\boldsymbol{I} + \mu \left[\nabla \boldsymbol{u} + \left(\nabla \boldsymbol{u} \right)^T \right] - \frac{2}{3} \mu \left(\nabla \cdot \boldsymbol{u} \right) \boldsymbol{I} \right\} + F, \tag{7}$$

$$\nabla \times \boldsymbol{H} = \boldsymbol{J}_e, \tag{8}$$

$$\boldsymbol{B} = \nabla \times \boldsymbol{A}, \tag{9}$$

$$\boldsymbol{J}_e = \frac{NI_{coil}}{A} \boldsymbol{e}_{coil} . \tag{10}$$

Here, Eq. (6) is the continuity equation for a fluid and Eq. (7) is the motion differential equation for an ideal fluid. In these two equations, ρ is the density of the fluid, u is the velocity vector of the fluid, I is the surface area vector of an ideal microelement fluidic hexahedron, μ is the fluid kinematic viscosity coefficient, and F and p are the force vector and pressure acting on the ideal microelement fluidic hexahedron, respectively. Equation (8) is the differential form of the law of the whole current, which means that the rotation of the magnetic strength $\boldsymbol{H}$ is equal to the conduction current density $\boldsymbol{J}_e$, expressed as Eq. (10). Equation (9) is the differential form of the magnetic field produced by the current. $\boldsymbol{A}$ is the integration of electric field. N is the number of turns of the coil and I_{coil} is the current in the coil. A is the area of the conductor.

The 3D model setup is shown in Fig. 2(a). The microfluidic channel is a cross-sectional cubic structure (800 μm wide, 200 μm thick, and 6 mm long) and is placed 20 mm away from the central axis and 20 mm above the top surface of the magnetic coil constructed using copper material (360 turns, 75 mm outside diameter, 20 mm inside diameter, and 20 mm height). An alternating current input into the coil is sinusoidal with a frequency of 50 Hz and an amplification of 5 A. An ellipsoid in the Fe_3O_4 magnetic material with a major axis length of 25 μm and a minor axis length of 5 μm is modeled for the MNP aggregation in the microfluidic channel. The simulation is carried out with a two-cycle time, i.e., 0.04 s, as shown in Figs. 2(b)–2(f). Figures 2(b) and 2(c) show that the force and torque acting on the aggregation are almost sinusoidal in three directions with a frequency of about 50 Hz. This occurs with little amplification of the three components, which indicates a primarily stable magnetic force and magnetic torque. The force will push the aggregation to move in a three-dimensional space. Figure 2(d) shows the linear relationship between the rotation angle and the time after 0.18 s. This suggests that the rotation speed of the aggregation is about 50 rad/s under an oscillating magnetic field of 50 Hz and 1147 A/m. From Fig. 2(e), a vortex with the highest flow velocity of 5.03 μm/s in the center portion of the aggregation is formed with the aggregation rotation speed of 50 rad/s around its major axis. Figure 2(f) shows the distribution of the flow stress on the surface of the object, which causes the deformation of the aggregation. The greatest pressure exists at the two ends of the major axis.

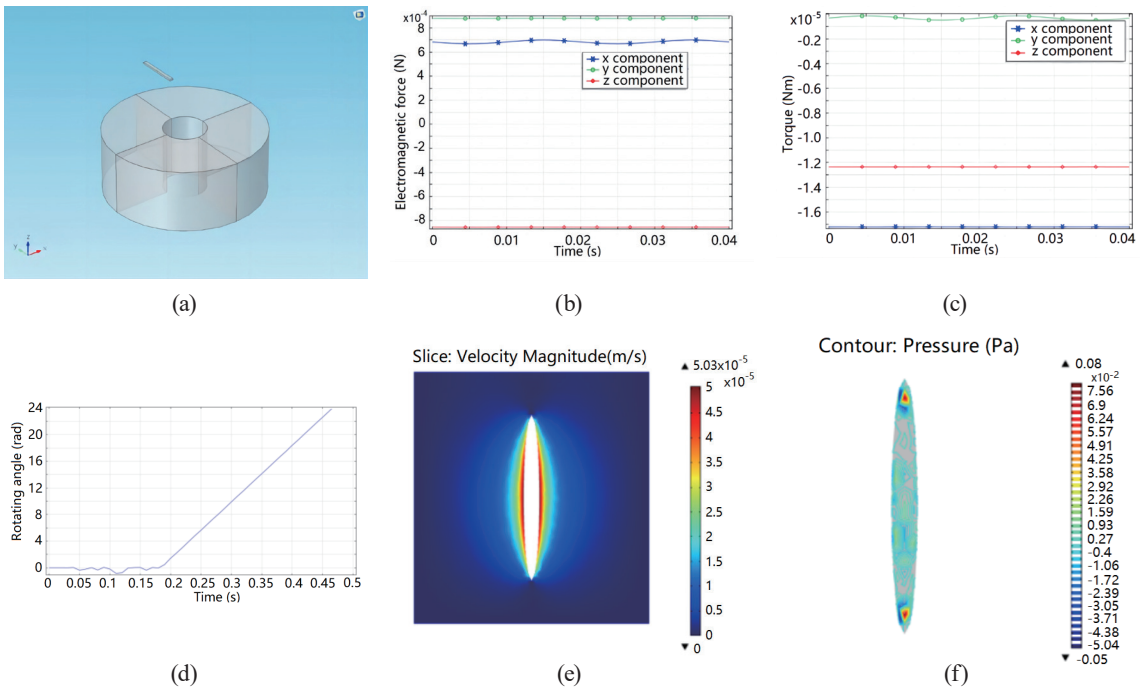

Fig. 2. (Color online) (a) Model setup for magnetic field and flow field analyses of MNPs in a microfluidic channel. (b) *x*, *y*, and *z* components of magnetic force applied on aggregation. (c) *x*, *y*, and *z* components of magnetic torque applied on aggregation. (d) Rotation angle varies with time (oscillating magnetic field of 50 Hz and 1147 A/m). (e) Velocity of vortex induced by aggregation with angular velocity of 50 rad/s. (f) Flow pressure applied on surface of aggregation.

3.2 Loss of fluid pressure in bend

Microfluidic channels of 0.8 mm diameter with angles from 0 to 90° in steps of 15° were used in this study. The length of the microfluidic channel was 3 mm with a flow velocity of 5 μm/s. Two points *M* and *N* upstream and downstream of the bend were chosen for the pressure measurement, and the difference between the two values is the pressure loss. Assuming that the length of *MN* with the angle of 0° is zero, the pressure loss is zero. The pressure distribution of flow in the microfluidic channel is shown in Fig. 3(a). The variation of the pressure loss coefficient with the angle and diameter is plotted in Fig. 3(b). It shows a pressure loss coefficient of 8.3×10^3.

4. Experimental Procedure

4.1 Synthesis of UK-coated Fe_3O_4 NPs

The Fe_3O_4 NPs were prepared by the coprecipitation method and subsequently coated with agarose gel on the surface to form agar@Fe_3O_4 NPs. UK was immobilized on agar@Fe_3O_4 NPs by the covalent binding method. The fundamental principle is that the carboxyl functional group (–COOH) of the agarose gel reacts with the amino group ($–NH_2$) via EDC/sulfo-NHS. The agar@Fe_3O_4 was prepared before the UK coating on the NPs. 2 g of agar powder was dissolved in 100 ml of deionized water to make 2% agar/H_2O solution. Then, a heated stirrer was used to stir and heat the solution for 1 h. Afterwards, the agar gel was obtained after the solution was cooled to room temperature. The agar gel was then immersed in a solution of 0.5 M $FeCl_2$ and 1 M $FeCl_3$ for 12 h. The agar gel was washed twice with deionized water and placed in a solution of 2.5 M/L sodium hydroxide for 30 min. The agar gel was washed five times with deionized water and placed in an oven at 70 °C for 24 h. The agar@Fe_3O_4 was obtained in powder form by grinding the dried gels with an agate mortar. Then, the NPs were coated with UK. First, 0.4 mM

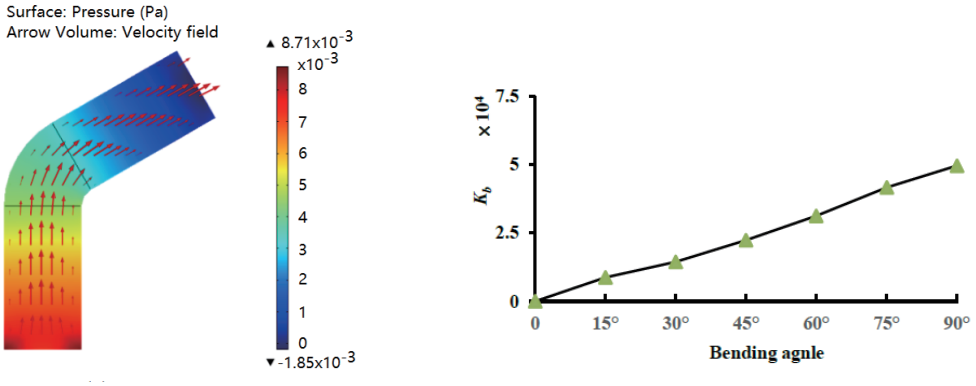

(a) (b)

Fig. 3. (Color online) (a) Pressure distribution of flow in microfluidic channel with an inflow velocity of 5 μm/s; arrows represent the flow direction. (b) Variation of pressure loss coefficient in bend *MN* every 15°.

EDC solutions and 100 mM sulfo-NHS were mixed and stirred for 5 min to obtain carrier-activated EDC/sulfo-NHS. 2% Agar@Fe_3O_4 suspensions were prepared and disrupted into the nanometer level with an ultrasonic disrupter. Then, the NPs were accumulated at the bottom of the container, whereas the supernatant was discarded. The surface-activated agar@Fe_3O_4 was obtained after washing twice. The active NPs were added into 10 ml of the UK solution, which was slightly alkaline, for 30 min. The UK-coated NPs were acquired after separation from the solution with a permanent magnet and placed at a temperature of 4 °C to keep the enzyme activated.

4.2 Preparation of microfluidic channel

The microfluidic channels are prepared from polydimethylsiloxane (PDMS) by lithography. Microfluidic channels with different diameters and bending angles were designed and are shown in Fig. 4. The relationship between the diameter and angle of the channel is shown in Table 1. The depth h of the microfluidic channels is 250 μm. In Table 1, the check and X marks represent the existence and nonexistence of the corresponding microfluidic channel sizes, respectively.

4.3 Preparation of thrombus sample

Pig blood was collected and placed in polyethylene tubes. After adding a coagulant, the tubes were refrigerated at 4 °C for 24 h. The clot was removed from the tubes and cut into pieces with approximately the same mass of 10.00 ± 0.01 mg. The mass was determined with a microbalance.

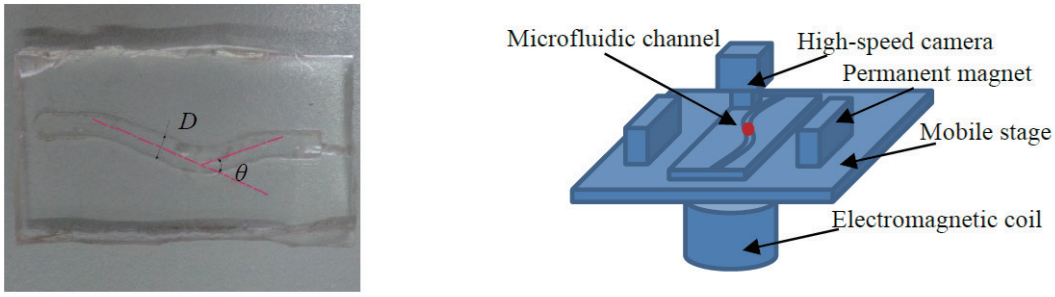

(a) (b)

Fig. 4. (Color online) (a) Designed microfluidic channel. (b) *In vitro* magnetically controlled thrombolysis system.

Table 1
Diameters and angles of microfluidic channels.

	0°	30°	60°	90°
0.8 mm	√	√	√	√
1.2 mm	√	×	×	×
2 mm	√	×	×	×
2.8 mm	√	×	×	×

4.4 *In vitro* thrombolysis device

The thrombolysis and efficiency measurement experiment was undertaken *in vitro* in a device with an electromagnetic coil, two permanent magnets ($Nd_2Fe_{14}B$, 32 × 14 × 4 mm^3; 0.35 T at the surface), and a high-speed camera (X-Stream Vision XS-3, IDT, United Kingdom), as shown in Fig. 4(b). A microfluidic channel was set between the two permanent magnets at a distance of 4 cm from each other. At this distance, the magnetic field applied to the microfluidic channel was measured to be 0.067 T with a Gauss/Tesla meter (FWBELL 5180, USA). The two permanent magnets and microfluidic channel were placed on a mobile stage. An electromagnetic coil fabricated from copper with insulation outside was placed under the stage. An alternating current was passed into the coil by a programmable AC power supply. The number of turns of the coil was 360 with a wire diameter of 1.25 mm. Also, in this experiment, a programmable microinjection pump system (not shown in the figure) was used to mimic the flow of the blood and inject the UK-coated MNPs.

5. Results and Discussion

5.1 Characteristics of prepared functionalized MNPs

Agar@Fe_3O_4 and UK-coated NPs were observed by transmission electron microscopy (TEM) (JOEL JEM-2010, JOEL, Tokyo, Japan), as shown in Figs. 5(a) and 5(b), the insets of

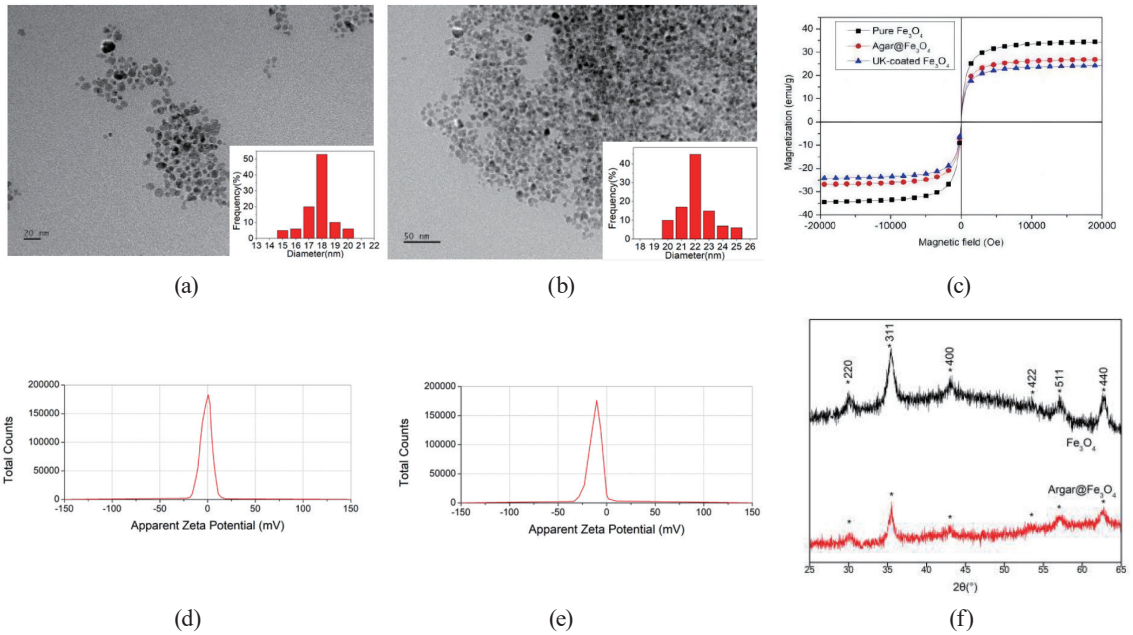

Fig. 5. (Color online) Characteristics of prepared Fe_3O_4 NPs. (a) TEM image and DLS results of agar@Fe_3O_4 NPs. (b) TEM image and DLS results of UK-coated Fe_3O_4 NPs. (c) VSM results of pure Fe_3O_4, agar@ Fe_3O_4, and UK-coated Fe_3O_4 NPs. (d) Zeta potential of UK-coated Fe_3O_4 NPs. (e) Zeta potential of UK-coated Fe_3O_4 NPs. (f) XRD results of pure Fe_3O_4 and agar@Fe_3O_4.

which are the results obtained with a dynamic light scattering (DLS) particle size distribution analyzer (LB-550, Horiba, Japan). Figure 5(a) shows that the size of the agar@Fe_3O_4 NPs is about 15–20 nm, and Fig. 5(b) shows that the size of the UK-coated Fe_3O_4 NPs is about 20–25 nm. A vibrating sample magnetometer (VSM) (JDM-13, Jilin University, Jilin, China) was used to determine the magnetization of the prepared Fe_3O_4 NPs. In Fig. 5(c), the saturation magnetism of pure Fe_3O_4 NPs is 35.1 emu/g, and the value decreases to 27.8 emu/g when coated by agar and 25.4 emu/g when further coated by UK. To further ensure that the UK is coated onto the surfaces of MNPs, the zeta potential was measured and is shown in Figs. 5(d) and 5(e). The zeta potentials of agar@Fe_3O_4 and UK-coated Fe_3O_4 NPs are 0.052 and −10.25 mV, respectively. A clear change in charge is the result of the coating of UK on the surface. XRD is used to analyze the structure and crystalline status of the material. There are five characteristic peaks of Fe_3O_4; their 2θ values are 30.1, 35.4, 43.1, 56.9, and 62.5°, which are shown in Fig. 5(f). The corresponding lattice planes are (220), (311), (400), (422), (511), and (440). The XRD pattern is identical to that of pure magnetite (JCPDS No. 82-1533), which indicates a cubic crystal system of the sample.

5.2 *In vitro* experiment

Four *in vitro* experiments in microfluidic channels were carried out to investigate the factors that affect the efficiency of thrombolysis using UK-coated Fe_3O_4 NPs. In each experiment, the same 12 mg thrombus sample was placed in the microfluidic channel. Then, deionized water with UK-coated MNPs was injected into the channel from one side using a microinjection pump. Then, the MNPs were manipulated by an oscillating magnetic field for microablation. The whole thrombolysis process was observed with a high-speed camera. Because it is too difficult to observe the MNPs owing to their nanoscale sizes, the whole thrombolysis process was observed at 10× magnification for a larger field of view.

The first experiment was carried out in microfluidic channels with a diameter of 0.8 mm and bending angles ranging from 0 to 90° every 30°. As discussed in Sect. 3.2, the bending angles have a significant impact on the fluid pressure loss. Such a loss may also result in the low pressure on the thrombus and affect the thrombolysis efficiency. A magnetic field strength of 624 A/m applied to the center of the microfluidic channel produced by an electromagnetic coil was used in the experiment. The image sequence in Fig. 6 shows the thrombolysis using the UK-coated MNPs in the microfluidic channel with a bending angle of 30°. As seen, the thrombus reduction was negligible before 60 s. Only those close to the exterior wall of the bend started to be ablated. This phenomenon is different from that in the straight channel starting from the center. The whole process was ended in 190 s. The result in Fig. 7(a) shows that for every 30° increase in the bending angle range from 0 to 90°, a thrombolysis efficiency decrease of about 0.25 mg/min is observed because the vortex force applied to the thrombi is weakened by the bend. However, the efficiency of thrombolysis using UK-coated MNPs is still 35% higher than that using pure UK.

The second experiment was on the effect of the diameter of the microfluidic channel on the thrombolysis efficiency. It was carried out in straight microfluidic channels with diameters of 0.8, 1.2, 2.0, and 2.8 mm. A contrast experiment with pure UK was carried out using the same

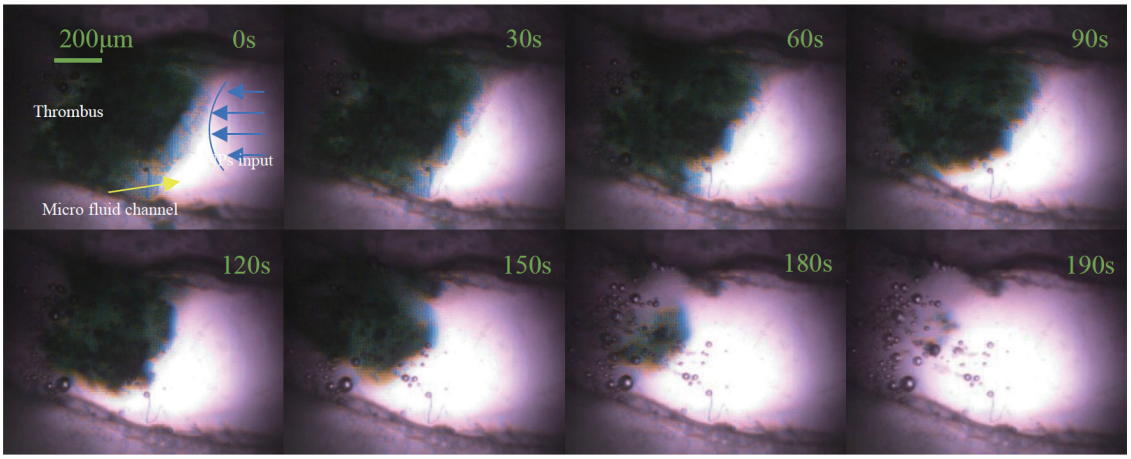

Fig. 6. (Color online) Thrombolysis by magnetically controlled UK-coated MNPs in a microfluidic channel with a bending angle of 30°.

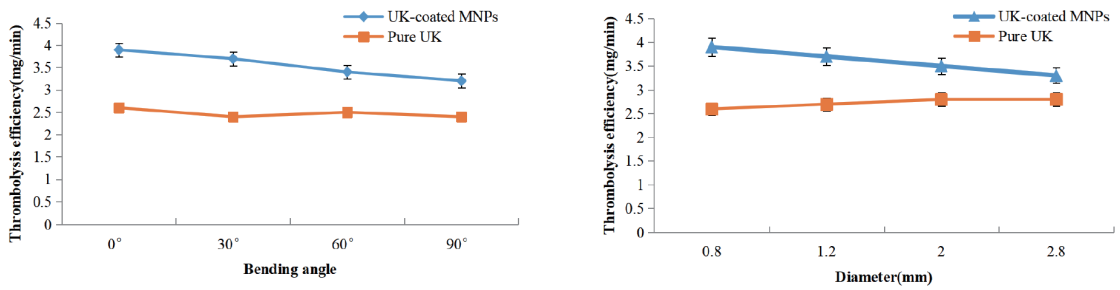

Fig. 7. (Color online) Thrombolysis efficiency varies with (a) bending angle and (b) diameter of microfluidic channel.

experiment station as the first experiment. Figure 7(b) shows that the efficiency of thrombolysis using the pure UK changed negligibly and was maintained at a level of 0.15 mg/min, whereas that using the UK-coated MNPs increased with decreasing diameter of the microfluidic channel. Such a phenomenon could be explained by the breaking force of MNPs. As the diameter decreased, more MNPs were attracted by the permanent magnet to accumulate in a narrow space. Thus, the fluidic vortex induced by the rotation of MNPs under an oscillating magnetic field would be strengthened to break the thrombus, and this accelerated the thrombolysis process. In the case of the pure UK without MNPs, as the amount of UK was fixed, the thrombolysis efficiency would not change considerably. As the internal diameter of many blood vessels in the heart is very small, a small occlusion will result in serious consequences. The acceleration of thrombolysis in a narrow channel with functionalized MNPs will be meaningful.

The third and fourth experiments were on the effects of mass fraction and magnetic strength on thrombolysis efficiency, respectively. Figure 8(a) shows thrombolysis efficiency as a function of four values of the mass fractions of UK-coated MNPs and pure UK. The UK-coated MNPs and pure UK solutions with mass fractions of 0.1, 0.3, 0.5, and 0.7% in the same volume of 50 ml

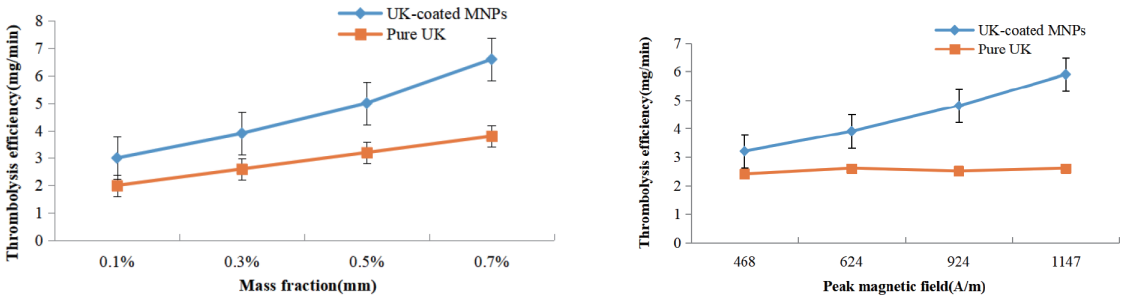

(a) (b)

Fig. 8. (Color online) Thrombolysis efficiency varies with (a) mass fraction and (b) peak magnetic field.

were mixed with 10 mg of the prepared thrombus in a bottle. The experiment was carried out under a magnetic strength H of 642 A/m produced by an electromagnetic coil. A clear efficiency increase with increasing mass fraction was observed. However, the thrombolysis efficiency is notably higher with UK-coated MNPs than with the pure UK. The figure also suggests that the rate of increase is higher with UK-coated MNPs than with the pure UK. As shown in Fig. 8(b), for a mass fraction of 0.3%, the efficiency of thrombolysis using UK-coated MNPs is further improved with the application of a magnetic field with increasing strength. The increasing trend of thrombolysis as a function of mass fraction and magnetic strength can be rationalized through the mechanism described in Sect. 2. The rotational speed of MNPs will increase with the magnetic strength as described by Eq. (3). In a colloidal ferrofluid, the magnetic susceptibility $\Delta\chi$ can be written as[16]

$$\Delta\chi = \varphi' M_b \frac{dL_\beta}{dH}, \tag{12}$$

where L_β is the Langevin function, M_b is the domain magnetization, and φ' is the volume fraction. Equation (12) reveals that the magnetic susceptibility is proportional to the volume fraction under a constant magnetic field. An increase in the MNP fraction will lead to an increase in the space gradient of the magnetic susceptibility. Thus, an enhanced breaking force will be applied to the thrombus, accelerating the thrombolysis rate.

6. Conclusions

The UK-coated MNPs in an oscillating magnetic field improve the efficiency of thrombolysis compared with pure UK *in vitro*. With good compatibility and a noncontact control advantage, the UK-coated MNPs are desired to be used clinically in the future. In this study, four factors that may affect the efficiency of thrombolysis were analyzed, namely, microfluidic channel bending, channel diameter, mass fraction, and peak strength of the oscillating magnetic field in windings. Compared with the factors of the vessel itself, the mass fraction and oscillating field have more obvious effects on the thrombolysis rate. However, noncontact method with an

increased strength of the oscillating magnetic field will be a feasible alternative in future clinical settings. The analysis of these factors will help determine the thrombolysis efficiency and help doctors make the right choices.

Acknowledgments

The authors gratefully acknowledge the support of the School of Mechanical Engineering, University of Shanghai for Science and Technology, Shanghai, China.

References

1 F. Scherer, U. Schillinger, J. Henke, C. Bergemann, A. Kruger, B. Gansbacher, and C. Plank: Eur. Cells. Mater. **3** (2002) 79. https://doi.org/10.1038/sj.gt.3301624
2 A. Jordan, R Scholz, K. Maier-Hauff, M. Johannsen, P. Wust, J. Nadobny, S. Hermann, S. Helmut, D. Serdar, L. Stefan, L. Wolfgang, and F. Roland: J. Magn. Magn. Mater. **225** (2001) 118. https://doi.org/10.1016/S0304-8853(00)01239-7
3 S. Kayal, D. Bandyopadhyay, T. K. Mandal, and R. V. Ramanujan: RSC Adv. **1** (2011) 238. https://doi.org/10.1039/C1RA00023C
4 A. S. Lubbe, C. Alexiou, and C. Bergemann: J. Surg. Res. **95** (2001) 200. https://doi.org/10.1006/jsre.2000.6030
5 J. L. F. Gabayno, D. W. Liu, and M. Chang: Nanoscale **7** (2015) 3947. https://doi.org/10.1039/c4nr06143h
6 C. C. Berry and A. S. G. Curtis: J. Phys. D: Appl. Phys. **36** (2003) 198. https://doi.org/10.1088/0022-3727/36/13/203
7 J. Cao, Y. Wang, J. Yu, J. Xia, C. Zhang, D. Yin, and U. O. Hafeli: J. Magn. Magn. Mater. **277** (2004) 165. https://doi.org/10.1016/j.jmmm.2003.10.022
8 A. D. Grief and G. Richardson: J. Magn. Magn. Mater. **293** (2005) 455. https://doi.org/10.1016/j.jmmm.2005.02.040
9 M. O. Aviles, A. D. Ebner, and J. A. Ritter: J. Magn. Magn. Mater. **310** (2007) 131. https://doi.org/10.1016/j.jmmm.2006.08.009
10 A. Banerjee, Y. Chisti, and U. C. Banerjee: Biotechnol. Adv. **22** (2004) 287 https://doi.org/10.1016/j.biotechadv.2003.09.004
11 M. Chang, Y. H. Lin, J. L. Gabayno, Q. Li, and X. Liu: Bioengineered **8** (2017) 29. https://doi.org/10.1080/21655979.2016.1227145
12 B. Feng, Z. Jing, Y. Su, Y. C. Tang, and J. N. Liu: Biomaterials **30** (2009) 5125. https://doi.org/10.1016/j.biomaterials.2009.06.006
13 Q. A. Pankhurst, J. Connolly, S. K. Jones, and J. Dobson: J. Phys. D: Appl. Phys. **36** (2009) 591. https://doi.org/10.1088/0022-3727/36/13/201
14 P. P. Modi and S. Jayanti: Chem. Eng. Res. Des. **82** (2004) 321. https://doi.org/10.1205/026387604322870435
15 A. Ward-Smith: Int. J. Heat Fluid Fl. **1** (1979) 123. https://doi.org/10.1016/0142-727X(79)90028-6
16 S. Boroun and F. Larachi: AIChE J. **63** (2016) 337. https://doi.org/10.1002/aic.15456